



# The rescue of F508del-CFTR by elexacaftor/tezacaftor/ivacaftor (Trikafta) in human airway epithelial cells is underestimated due to the presence of ivacaftor

Frédéric Becq<sup>1</sup>, Sandra Mirval<sup>1</sup>, Thomas Carrez<sup>1,2</sup>, Manuella Lévêque<sup>1</sup>, Arnaud Billet <sup>1</sup>, Christelle Coraux<sup>3</sup>, Edouard Sage<sup>4,5</sup> and Anne Cantereau<sup>1</sup>

<sup>1</sup>Laboratoire Signalisation et Transports Ioniques Membranaires, Université de Poitiers, Poitiers, France. <sup>2</sup>ManRos therapeutics, Presqu'île de Perharidy, Roscoff, France. <sup>3</sup>INSERM UMR-S 1250, Université de Reims-Champagne Ardenne, Reims, France. <sup>4</sup>INRAE UMR 0892, Université Versailles-Saint-Quentin-en-Yvelines, Versailles, France. <sup>5</sup>Service de Chirurgie Thoracique et Transplantation Pulmonaire, Hôpital Foch, Suresnes, France.

Corresponding author: Frédéric Becq ([frederic.becq@univ-poitiers.fr](mailto:frederic.becq@univ-poitiers.fr))



Shareable abstract (@ERSpublications)

**Ivacaftor is not able to potentiate the function of Trikafta-rescued F508del-CFTR due to its destabilising effect. Ivacaftor does not preclude the use of different potentiators combined with Trikafta, so the beneficial effect of Trikafta is underestimated.** <https://bit.ly/3dxlsJb>

**Cite this article as:** Becq F, Mirval S, Carrez T, *et al.* The rescue of F508del-CFTR by elexacaftor/tezacaftor/ivacaftor (Trikafta) in human airway epithelial cells is underestimated due to the presence of ivacaftor. *Eur Respir J* 2022; 59: 2100671 [DOI: 10.1183/13993003.00671-2021].

Copyright ©The authors 2022.  
For reproduction rights and  
permissions contact  
[permissions@ersnet.org](mailto:permissions@ersnet.org)

This article has an editorial  
commentary:  
[https://doi.org/10.1183/  
13993003.02380-2021](https://doi.org/10.1183/13993003.02380-2021)

Received: 5 March 2021  
Accepted: 25 June 2021

## Abstract

Trikafta, currently the leading therapeutic in cystic fibrosis (CF), has demonstrated a real clinical benefit. This treatment is the triple combination therapy of two folding correctors elexacaftor/tezacaftor (VX445/VX661) plus the gating potentiator ivacaftor (VX770). In this study, our aim was to compare the properties of F508del-CFTR in cells treated with either lumacaftor (VX809), tezacaftor, elexacaftor, elexacaftor/tezacaftor with or without ivacaftor. We studied F508del-CFTR function, maturation and membrane localisation by Ussing chamber and whole-cell patch-clamp recordings, Western blot and immunolocalisation experiments. With human primary airway epithelial cells and the cell lines CFBE and BHK expressing F508del, we found that, whereas the combination elexacaftor/tezacaftor/ivacaftor was efficient in rescuing F508del-CFTR abnormal maturation, apical membrane location and function, the presence of ivacaftor limits these effects. The basal F508del-CFTR short-circuit current was significantly increased by elexacaftor/tezacaftor/ivacaftor and elexacaftor/tezacaftor compared to other correctors and nontreated cells, an effect dependent on ivacaftor and cAMP. These results suggest that the level of the basal F508del-CFTR current might be a marker for correction efficacy in CF cells. When cells were treated with ivacaftor combined to any correctors, the F508del-CFTR current was unresponsive to the subsequently acute addition of ivacaftor, unlike the CFTR (cystic fibrosis transmembrane conductance regulator) potentiators genistein and Cact-A1 which increased elexacaftor/tezacaftor/ivacaftor and elexacaftor/tezacaftor-corrected F508del-CFTR currents. These findings show that ivacaftor reduces the correction efficacy of Trikafta. Thus, combining elexacaftor/tezacaftor with a different potentiator might improve the therapeutic efficacy for treating CF patients.

## Introduction

Cystic fibrosis (CF; MIM#219700), one of the most common, lethal and autosomal recessive diseases, is caused by mutations in the *CFTR* gene (MIM#602421) encoding the anion channel CFTR (cystic fibrosis transmembrane conductance regulator). CFTR is a key player in transepithelial fluid secretion [1]. A defect in its expression, apical location or function results in CF; a multisystem pathology with severe pulmonary (accumulation of thick, sticky mucus in the bronchi of the lungs) and digestive (loss of exocrine pancreatic function, impaired intestinal absorption) impairments [1]. The most common CF mutation, a deletion of phenylalanine at position 508 (F508del), is a class-2 mutation exhibiting inefficient maturation and reduced plasma membrane expression of the protein [2–4]. In addition, F508del-CFTR exhibits a gating

defect [5], reduced stability at the plasma membrane [6, 7] and thermal instability at physiological temperature [8, 9]. This mutation is present in ~85% and ~81% of individuals in the United States [10] and Europe [11], respectively. Overall, CF affects >31000 people in the United States [10] and almost 50000 people in 38 European countries [11].

It is now agreed that these F508del-defects cannot be addressed by a classical monotherapy, but by combination of modulators addressing single defects (*i.e.* correctors and potentiators acting respectively on protein maturation/folding and channel function) [12, 13]. Applying a single F508del-corrector such as VX809 (lumacaftor) [14] or VX661 (tezacaftor) has little efficiency, while combining them with the gating potentiator VX770 (ivacaftor) [15–17], leading to the marketed medicaments Orkambi and Symdeko, respectively, improves function, but with only a modest clinical benefit [18–21], possibly due to interference between corrector and potentiator compounds [22–24].

To overcome the limited efficacy of first-generation correctors, novel second-generation correctors were developed (table 1). This strategy gave birth to the triple combination elexacaftor/tezacaftor/ivacaftor (Trikafta, USA/Kaftrio, European Union) approved for treatment of CF patients aged  $\geq 12$  years with at least one F508del mutation in the CFTR protein [25–27]. Phase 3 clinical trials with Trikafta were conclusive, describing a better gain in lung function (augmented percentage predicted forced expiratory volume in 1 s and reduction in lung exacerbation) compared to Orkambi and Symdeko (table 1) and improvement in the quality of life of patients [25–27]. Moreover, Trikafta was also effective on rare misfolding mutants of CFTR such as S13F, R31C, G85E, E92 K, V520F, M1101 K and N1303 K [28, 29]. This suggests that Trikafta/Kaftrio might be prescribed to CF patients with at least one copy of the *CFTR* gene with one class 2 misfolding mutation.

Because few reports dissecting the functional recovery of F508del by Trikafta in airway epithelial cells are available, our aim was to study and compare in more detail the effects of the components of Trikafta with or without ivacaftor on the function, maturation and pharmacological properties of F508del-CFTR in human airway epithelial cells.

## Materials and methods

### Cell culture

Human airway epithelial (HAE) cells were obtained from the department of thoracic surgery and lung transplantation of the Foch hospital (Suresnes, France) from explanted CF lungs at the time of patient's transplantation [30]. Human tissues from three F508del/F508del donors were collected and used according to French law, with the informed consent of patients and through the authorisation of Biological Collection

TABLE 1 Therapeutic cystic fibrosis transmembrane conductance regulator modulators

	Market name USA/EU	Year Approved USA (FDA)/ EU (EMA)	Indication (age)	CF mutations	CF population %	Lung ppFEV <sub>1</sub>	Lung exacerbation reduction %	Estimated annual cost USD/EUR
<b>Ivacaftor</b>	Kalydeko	2012/2014	>6 months	Class III, gating mutation, residual function and conduction mutations (class IV)	3–5	10.6–12.5 (week 24)	55	311 000/260 000
<b>Lumacaftor/ ivacaftor</b>	Orkambi	2015/2018	>12 years >6 years	Class II, F508del homozygous	45–50	2.6–4.0	30–39	272 000/226 000
<b>Tezacaftor/ ivacaftor with ivacaftor</b>	Symdeko/ Symkevi	2018/2018	>6 years	Class II, F508del homozygous, heterozygous, other mutations	45–50	4.0–6.8	35	292 000/242 000
<b>Elexacaftor/ tezacaftor/ ivacaftor with ivacaftor</b>	Trikafta/ Kaftrio	2019/2020	>6 years	Class II, at least one copy of F508del mutation and one copy with residual function mutation	85–90	10.4–13.8	63	311 000/260 000

EU: European Union; FDA: Food and Drug Administration; EMA: European Medicines Agency; CF: cystic fibrosis; ppFEV<sub>1</sub>: percentage predicted forced expiratory volume in 1 s.

number DC-2012–1583 obtained from the French Ministry of Higher Education and Research, and with the approval number 21–775 of institutional review board 00003888. Airways were dissected and epithelial cells obtained after overnight enzymatic dissociation using  $0.5 \text{ mg}\cdot\text{mL}^{-1}$  pronase E (Sigma Aldrich, USA). Primary HAE cells were seeded on type IV collagen-coated dishes and cultured in Pneumacult™-Ex medium (StemCell Technologies, France) supplemented with tobramycin ( $80 \text{ }\mu\text{g}\cdot\text{mL}^{-1}$ ), ceftazidime ( $100 \text{ }\mu\text{g}\cdot\text{mL}^{-1}$ ), vancomycin ( $100 \text{ }\mu\text{g}\cdot\text{mL}^{-1}$ ), amphotericin B ( $0.25 \text{ }\mu\text{g}\cdot\text{mL}^{-1}$ ), penicillin ( $100 \text{ units}\cdot\text{mL}^{-1}$ ) and streptomycin ( $100 \text{ }\mu\text{g}\cdot\text{mL}^{-1}$ ) (Sigma Aldrich).

The human bronchial epithelial cell lines non-CF (CFBE41o<sup>-</sup> wild-type CFTR cells) and CF (CFBE41o<sup>-</sup> F508del-CFTR cells), provided by D. Gruenert (University of California San Francisco, CA, USA), were grown at 37°C in 5% carbon dioxide (CO<sub>2</sub>)–95% air and media were replaced every 2 days [30]. These cell lines were grown in Eagle's minimum essential medium containing nonessential amino acids (Gibco, USA) supplemented with 10% fetal bovine serum (FBS) (Eurobio, France), 2 mM L-glutamine, 50 units·mL<sup>-1</sup> penicillin, 50  $\mu\text{g}\cdot\text{mL}^{-1}$  streptomycin (Sigma Aldrich) and were selected using 5  $\mu\text{g}\cdot\text{mL}^{-1}$  puromycin (Gibco). F508del-CFTR proteins were restored to the plasma membrane by incubating cells with various combinations of VX445, VX661, VX809, VX770 over 24 h, prior to experiments.

The baby hamster kidney (BHK) cell line was cultured in DMEM/F12 medium supplemented with 5% FBS and 1% penicillin/streptomycin. To study F508del-CFTR chloride currents by patch clamp and protein maturation by Western blot, BHK were stably transfected with pNUT-F508del- or wild-type-CFTR plasmids using JetPeI reagent (Polyplus, France) according to the manufacturer's instructions. Clones were selected by addition of methotrexate (500  $\mu\text{M}$ ) and CFTR expression validated by immunoblotting.

#### Modulator treatment

F508del-CFTR expressing cells used in the present study were treated with modulators 24 h prior to the experiments. The following modulators (supplementary figure S1a) were used: VX809 (lumacaftor 3  $\mu\text{M}$ ), VX661 (tezacaftor 18  $\mu\text{M}$ ), VX445 (elexacaftor 3  $\mu\text{M}$ ), VX809/VX770 (Orkambi 3  $\mu\text{M}$  and 1  $\mu\text{M}$ ), VX661/VX770 (Symdeko 18  $\mu\text{M}$  and 1  $\mu\text{M}$ ), VX445/VX661 (3  $\mu\text{M}$  and 18  $\mu\text{M}$ ) and Trikafta composed of VX661 (18  $\mu\text{M}$ ) plus VX445 (3  $\mu\text{M}$ ) plus VX770 (1  $\mu\text{M}$ ). In our study, we selected the concentrations used by KEATING *et al.* [25] describing the *in vitro* effect of these compounds on CF airway epithelial cells; VX661 at the concentration of 18  $\mu\text{M}$ , VX445 at 3  $\mu\text{M}$  and VX770 at 1  $\mu\text{M}$ . In some experiments we also used VX809 (3  $\mu\text{M}$ ) instead of VX661 in the triple combination of VX809/VX445/VX770.

#### Short-circuit current measurements

HAE cells from distinct F508del/F508del donors were seeded at a density of  $0.1\times 10^6$  cells on type IV collagen-coated Snapwell permeable inserts (Corning, USA), as described [30]. They were cultured in liquid/liquid conditions in Pneumacult-Ex medium for 5–7 days until confluence was reached and then at air/liquid interface for 21–28 days. The culture medium was composed of 1:1 DMEM/F12 (Gibco) and bronchial epithelial cell growth medium (Lonza, Switzerland) with the Lonza supplements for human epithelial growth factor, epinephrine, bovine pituitary extract, hydrocortisone, insulin, tri-iodothyronine and transferrin. Finally, the culture medium was supplemented with 50 units·mL<sup>-1</sup> penicillin (Sigma Aldrich), 50  $\mu\text{g}\cdot\text{mL}^{-1}$  streptomycin (Sigma Aldrich), 0.1 nM retinoic acid (Sigma Aldrich) and 1.5  $\mu\text{g}\cdot\text{mL}^{-1}$  bovine serum albumin (Sigma Aldrich). The CFBE epithelial cells were seeded at a density of  $0.5\times 10^6$  cells on Snapwell permeable inserts (Corning) coated with 5  $\mu\text{g}\cdot\text{cm}^{-2}$  human fibronectin (Sigma Aldrich) as described in [30]. After 2 days at the liquid/liquid interface, cells were cultured at the air/liquid interface. The transepithelial resistance of our HAE cultures and CFBE F508del reached a minimum of  $\sim 1100$ – $1900 \text{ }\Omega\cdot\text{cm}^{-2}$  and  $\sim 400$ – $500 \text{ }\Omega\cdot\text{cm}^{-2}$ , respectively, as measured with a Millicell-ERS voltmeter-ohmmeter (Merck Millipore, USA) on the day of the Ussing experiment.

Inserts containing pseudo-epithelia were then mounted in an EM-CSYS-6 nonperfused Ussing chamber system (Physiologic Instruments, USA) composed of two hemi-chambers, each containing a different solution. Asymmetric solutions were used, creating a basal to apical chloride gradient to enhance chloride current detection. Their compositions were (in mM): 1.2 NaCl, 115 Na-gluconate, 25 NaHCO<sub>3</sub>, 1.2 MgCl<sub>2</sub>, 4 CaCl<sub>2</sub>, 2.4 KH<sub>2</sub>PO<sub>4</sub>, 1.24 K<sub>2</sub>HPO<sub>4</sub>, 10 mannitol (pH 7.4) for apical solution and 115 NaCl, 25 NaHCO<sub>3</sub>, 1.2 MgCl<sub>2</sub>, 1.2 CaCl<sub>2</sub>, 2.4 KH<sub>2</sub>PO<sub>4</sub>, 1.24 K<sub>2</sub>HPO<sub>4</sub>, 10 glucose (pH 7.4) for basal solution. Apical and basal solutions were maintained at 37°C (controlled before and after each experiment) and gassed with 95% oxygen–5% CO<sub>2</sub>. Transepithelial potential difference and short-circuit currents (*I*<sub>sc</sub>) were measured/injected through 3 M KCl-filled Ag/AgCl electrodes connected to a VCC MC2 voltage/current clamp (Physiologic Instruments). Visualisation and recording of the current injected by the system to short-circuit pseudo-epithelia (clamp at 0 mV) was visualised and recorded at a frequency of 0.1 Hz on a personal computer using Acquire and Analyse hardware and software (Physiologic Instruments).

Transepithelial potential differences were corrected for the junction potential between apical and basal solutions and for empty insert resistance. Since the polarity of  $I_{sc}$  was referred to the basal side of the pseudo-epithelium and a gain of  $-10$  was applied, an apical anion secretion was indicated by an increase in  $I_{sc}$ .

Supplementary figure S1b shows the assay protocol for the activation and inhibition of F508del-CFTR mediated chloride currents recorded in our cell models. Pharmacological reagents were added to the apical bathing solution. In all experiments, the transepithelial F508del-CFTR current ( $I_{sc}$ ) was assessed after blocking sodium currents by amiloride ( $100\ \mu\text{M}$ ) and 15 min later, CFTR activation was induced by various agonists (forskolin, VX770, Genistein [31] and Cact-A1 [32]). To inhibit CFTR-specific chloride secretion, we added either CFTR-inh172 ( $10\ \mu\text{M}$ ) [33] or GlyH-101 ( $15\ \mu\text{M}$ ) [34]. Adding UTP ( $100\ \mu\text{M}$ , not illustrated) after CFTR inhibition was used to control calcium-activated chloride channel activity and integrity of the cells at the end of experiments. Supplementary figure S1c illustrates our analysis of  $I_{sc}$ . We recorded the basal current obtained after stability of the  $I_{sc}$ , that is reached 5–15 min after adding amiloride. After 15 min we measured the forskolin- and/or potentiator-dependent delta  $I_{sc}$  and finally the change ( $\Delta$ )  $I_{sc}$  after blocking CFTR.

#### *Patch-clamp experiments*

The BHK cell line stably expressing F508del-CFTR was used for the patch-clamp experiments, essentially as described in [35]. Automated whole-cell patch clamp was performed on the eight-channel Patchliner NPC-16 workstation (Nanion Technologies, Munich, Germany), which was coupled to two QuadroEPC-10 amplifiers (HEKA Elektronik, Germany). Our procedures followed Nanion's standards and used Nanion's high resistance chips (resistances of 3–3.5 M $\Omega$ ). To record CFTR currents, pulses from the holding potential of  $-40\ \text{mV}$  to test potentials between  $-80$  and  $+80\ \text{mV}$  in 20-mV increments were used. Results were expressed as the current density/voltage [35]. The external bath solution contained (in mM): 145 NMDG, 145 HCl, 10 TES, 5 BaCl<sub>2</sub>, 2 CaCl<sub>2</sub>, 2 MgCl<sub>2</sub> (titrated with NMDG to pH 7.4). The osmolarity of the bath solution was  $300\pm 10\ \text{mOsmol}$ . The internal solution contained (in mM): 105 NMDG, 30 H<sub>2</sub>SO<sub>4</sub>, 20 HCl, 10 TES, 10 EGTA, 4 MgCl<sub>2</sub> and 3 MgATP titrated to pH 7.2 with HCl. Osmolarity of the pipette solution was  $285\pm 5\ \text{mOsmol}$ . A theoretical  $E_{\text{Cl}^-}$  of  $-44\ \text{mV}$  was determined with the Nernst equation. Recordings were performed at room temperature (20–25 °C). Results were analysed with Patch MasterPro software (HEKA Elektronik).

#### *Western blotting*

To determine CFTR expression, CFBE F508del-CFTR, CFBE wild-type CFTR, BHK cells stably expressing F508del-CFTR or wild-type CFTR were lysed using a lysis buffer containing 10 mM Tris HCl, 1% Nonidet P-40, 0.5% sodium deoxycholate, 1 mM Pefabloc SC (Sigma Aldrich) and the protease inhibitors cocktail Complete (Roche, Germany). Next, protein extracts were quantified using BCA kit (Pierce) and 50  $\mu\text{g}$  of protein samples were separated on sodium dodecyl sulphate–polyacrylamide gel electrophoresis (SDS-PAGE) (7%) and transferred to a nitrocellulose membrane. The membrane was then subjected to Western blotting using a mouse anti-CFTR antibody (MAB3480, aa 1370–1380, clone M3A7, 1:1000; Merck Millipore, USA) [36] and a mouse anti-Na<sup>+</sup>/K<sup>+</sup> ATPase (1:1000; SantaCruz Biotechnology, USA). Horseradish peroxidase-conjugated sheep anti-mouse antibody (1:5000; GE Healthcare, UK) was used as secondary antibody, and proteins were detected using enhanced chemiluminescence (Immobilon; Merck Millipore, France). Images were obtained using the GeneGnome Imager (SynGene Ozyme, France) and analysed for densitometry with the Genetools software (SynGene Ozyme). The intensity of the bands was normalised to the loading control, the Na<sup>+</sup>/K<sup>+</sup> ATPase protein and CFTR maturation status was estimated by the band B/(band B+band C) ratio. The Rainbow molecular weight markers (Amersham, USA) have been used for identification of proteins on SDS-polyacrylamide gels.

#### *Immunofluorescence*

At the end of the Ussing experiments, CFBE cells were directly fixed in the insert using 3% paraformaldehyde for 10 min, and conserved at 4°C until immunostaining. Then, cells were permeabilised for 5 min with 0.1% Triton X-100 diluted in PBS and incubated with a mouse anti-human CFTR antibody (MAB25031, aa 1377–1480, Clone # 24–1, 1:400, Bio-Techne, USA) blocked with 1% bovine serum albumin (Sigma Aldrich) for 2 h at room temperature. After three 5-min washes, cells were incubated with Alexa Fluor™ 647-conjugated donkey anti-mouse antibody (AF647, 1:200; Invitrogen, USA) for 1 h and rinsed again three times. Immunostaining was followed by 5-min staining of the cell nuclei with diamidino-phenyl-indole (DAPI, 1:1000, Sigma Aldrich). Each filter was then detached from its insert under binocular loupe with a scalpel blade and mounted using Mowiol within a microscope slide and coverslip (Menzel-Gläser, Sigma Aldrich).

### Confocal imaging and analysis

A FV3000 confocal microscope (Olympus, France) was used to acquire high-resolution three-dimensional (3D) images with  $\times 60/1.40$  oil objective (UPLXAPOXO). 405 nm and 640 nm laser lines were used for detection of DAPI (Em $\lambda$ : 430–470 nm) and AlexaFluor 647 (Em $\lambda$ : 650–750 nm). Z-stack images were acquired with 0.2 stepsize through the entire depth of the sample. Z sections were obtained with Imaris software (Bitplane, Oxford Instruments, UK). 3D images were also analysed using Fiji software. First quantification of CFTR staining was performed on maximum intensity projection images. A minimum of 15 regions of interest (ROI) were defined on each field with contrast enhancing if needed (but not applied) in order to identify significant number of cells throughout the image (five images per condition). The experiment was repeated twice on two different cell cultures. As a second analysis, a study of CFTR staining along the z-axis was done with the same ROI defined as previously described for quantification. Data were analysed using Excel software. For all the 15 ROIs per image, mean values obtained along the z-axis (0.2  $\mu$ m step) were manually aligned on AF647 peak intensity and mean curve generated for each image. Mean curves of five images were then treated in the same manner to align their AF647 peak value and final mean curve was calculated. Values from the DAPI channel followed AF647 Z realignment and was treated as AF647 signal to calculate global mean and normalised.

### Chemicals

Amiloride, UTP, forskolin, genistein, MK571 were from Sigma (Sigma Aldrich, USA). The selective CFTR inhibitors CFTR<sub>inh</sub>172 and GlyH101 and the CFTR activator Cact-A1 (5-((Z)-2-(2-(allyloxy)phenyl)-1-cyanovinyl)-3-amino-1H-pyrazole-4-carbonitrile, (Z)-3-(2-(2-(allyloxy)phenyl)-1-cyanovinyl)-5-amino-1H-pyrazole-4-carbonitrile) were from Calbiochem (Calbiochem, USA). The following compounds were from Selleckchem (Selleck Chemicals, USA) (International Union of Pure and Applied Chemistry name): VX445 (elxacaftor), (*N*-(1,3-dimethylpyrazol-4-yl)sulfonyl-6-(3-(3,3,3-trifluoro-2,2-dimethylpropoxy)pyrazol-1-yl)-2-((4*S*)-2,2,4-trimethylpyrrolidin-1-yl)pyridine-3-carboxamide); VX661 (tezacaftor), (1-(2,2-difluoro-1,3-benzodioxol-5-yl)-*N*-(1-((2*R*)-2,3-dihydroxypropyl)-6-fluoro-2-(1-hydroxy-2-methylpropan-2-yl)indol-5-yl)cyclopropane-1-carboxamide); VX770 (ivacaftor), (*N*-(2,4-ditert-butyl-5-hydroxyphenyl)-4-oxo-1*H*-quinoline-3-carboxamide); VX809 (lumacaftor), (3-(6-((1-(2,2-difluoro-1,3-benzodioxol-5-yl)cyclopropanecarbonyl)amino)-3-methylpyridin-2-yl)benzoic acid). Note that VX445 is not chiral purity and thus the manufacturer does not specify enantiomeric VX-445 forms (S, R). Stock solutions of these pharmacological agents were prepared in dimethyl sulfoxide (DMSO) to make a 1000-fold concentrated stock solution.

### Statistical analysis

Data are presented as mean $\pm$ SEM of *n* observations. Statistical comparisons were made using nonparametric (*n*<10) or parametric (*n* $\geq$ 10) tests with a significance level of 0.05. Before using a parametric test, samples were checked for normality using the Shapiro–Wilk normality test. Statistical significance was determined using the Mann–Whitney test using GraphPad Prism version 6.0 (GraphPad Software, San Diego, CA, USA) software. Differences were considered statistically significant at *p*<0.05.

## Results

### *Rescue of F508del-CFTR-dependent transepithelial currents in primary HAE cells by elxacaftor/tezacaftor with and without ivacaftor*

We recorded the F508del-CFTR-dependent *I*<sub>sc</sub> of primary HAE cells from F508del homozygous CF donors to evaluate the correction effect of the components of Trikafta, elxacaftor/tezacaftor/ivacaftor (or VX445/VX661/VX770 hereafter named 3VX) and elxacaftor/tezacaftor (hereafter named 2VX). In these experiments, *I*<sub>sc</sub> was first stimulated by forskolin (FSK; 1  $\mu$ M) and then by VX770 (1  $\mu$ M) and finally inhibited by CFTR<sub>inh</sub>172 (10  $\mu$ M). In control experiments with HAE incubated 24 h in DMSO, FSK and VX770 were not able to increase *I*<sub>sc</sub>, as shown figure 1a. In contrast, with HAE cells treated with either 2VX (figure 1b) or 3VX (figure 1c), adding FSK (1  $\mu$ M) rapidly increased *I*<sub>sc</sub> which then stabilised. We observed three differences with HAE cells treated with either 3VX or 2VX. First, the basal *I*<sub>sc</sub> level (before adding FSK) was significantly increased in the 3VX experimental condition compared to 2VX (*p*<0.001; figure 1d). Second, the *I*<sub>sc</sub> response to FSK was significantly increased for inserts treated with 3VX versus 2VX (*p*<0.001; figure 1e). Third, the FSK-activated *I*<sub>sc</sub> could not be further potentiated (*p*<0.01; figure 1f) by the acute addition of VX770 (figure 1b and c). However, as also shown figure 1c, adding a higher concentration of FSK after VX770 further increased *I*<sub>sc</sub> for 3VX-treated HAE cells showing that the chloride current was not maximal after VX770. In all experimental conditions, adding CFTR<sub>inh</sub>172 (10  $\mu$ M) rapidly inhibited *I*<sub>sc</sub>.

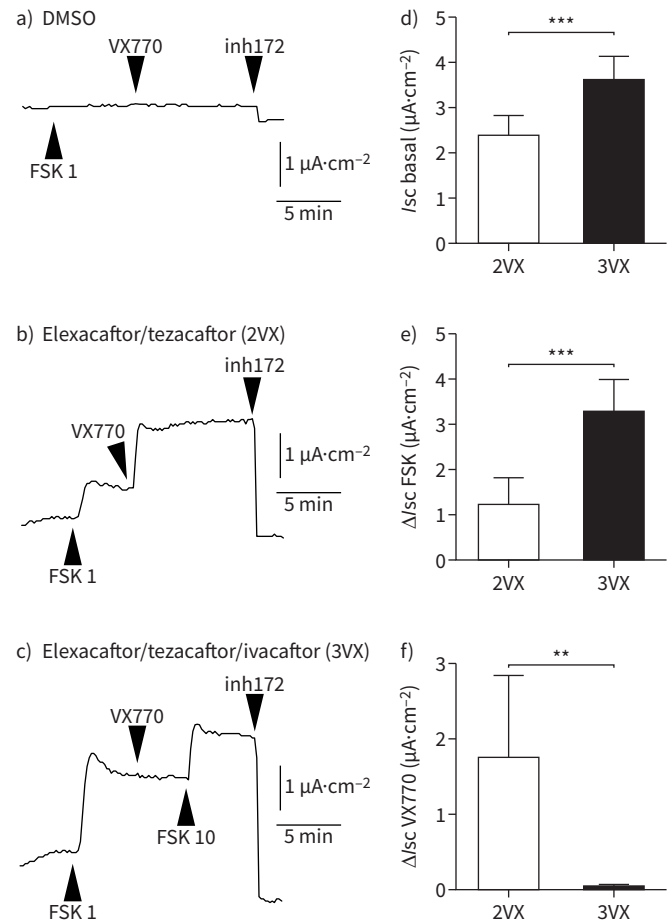


**FIGURE 1** Rescue of F508del short-circuit currents (Isc) in human airway epithelial (HAE) cells by elexacaftor/tezacaftor with or without ivacaftor. Original tracings of Isc as function of time for F508del-HAE cells incubated 24 h with a) dimethyl sulfoxide (DMSO); b) elexacaftor/tezacaftor (2VX); and c) the components of Trikafta, i.e. elexacaftor/tezacaftor/ivacaftor (3VX). F508del-CFTR (cystic fibrosis transmembrane conductance regulator) Isc was stimulated by forskolin (FSK) at 1 μM (FSK 1) and then 1 μM VX770 and finally inhibited by 10 μM CFTRinh172. d) Mean ± SEM of basal Isc for HAE cells treated with 2VX (n=6) and 3VX (n=7). e, f) Mean ± SEM of ΔIsc in the presence of e) FSK and f) VX770 for HAE cells treated with 2VX (n=6) and 3VX (n=7). \*\*: p < 0.01, \*\*\*: p < 0.001.

### The correctors elexacaftor and tezacaftor synergistically rescue F508del-CFTR function

In a second series of experiments (figure 2), we recorded F508del-CFTR Isc for CFBE F508del-CFTR epithelial cells incubated for 24 h with the individual correctors lumacaftor, tezacaftor, elexacaftor and with the combination of elexacaftor/tezacaftor (2VX) at the concentrations indicated in the method section. In each experiment, Isc was stimulated by FSK (1 μM) and then by VX770 (1 μM) and finally inhibited by CFTRinh172 (10 μM). The Isc recorded with cells treated with elexacaftor alone was significantly increased as compared to lumacaftor or tezacaftor. When we combined elexacaftor and tezacaftor (2VX) we recorded a higher Isc with either FSK or FSK+VX770 (figure 2a, b), in good agreement with previous reports [25, 28, 29]. Moreover, the values obtained show that the level of currents with the combination 2VX cannot be explained by the simple addition of the individual effects measured with elexacaftor or tezacaftor. Indeed, if we simply add the maximum Isc value reached after adding FSK+VX770 with cells treated with either elexacaftor (n=5,  $\Delta I_{sc_{VX445}} = 31 \pm 1.4 \mu A \cdot cm^{-2}$ ) or tezacaftor (n=11,  $\Delta I_{sc_{VX661}} = 7.6 \pm 0.75 \mu A \cdot cm^{-2}$ ), it gives a theoretical value  $< 40 \mu A \cdot cm^{-2}$ , whereas the experimental Isc value recorded with cells treated with elexacaftor/tezacaftor was  $\Delta I_{sc_{2VX}} = 69 \pm 3.5 \mu A \cdot cm^{-2}$  (n=14), indicating that elexacaftor and tezacaftor act synergistically and not additively to rescue F508del function (figure 2b). This is also the case with FSK alone ( $\Delta I_{sc_{VX661}} = 3.3 \pm 0.3 \mu A \cdot cm^{-2}$ , n=12;  $\Delta I_{sc_{VX445}} = 7.6 \pm 0.4 \mu A \cdot cm^{-2}$ , n=6; theoretical  $I_{sc_{2VX}} \sim 11 \mu A \cdot cm^{-2}$ ; experimental  $\Delta I_{sc_{2VX}} = 40 \pm 2.8 \mu A \cdot cm^{-2}$  (n=14, p < 0.0001 compared to  $I_{sc_{VX445}}$ ). This synergy has been reported previously [25, 28]. Finally, our conclusions are supported by the data on

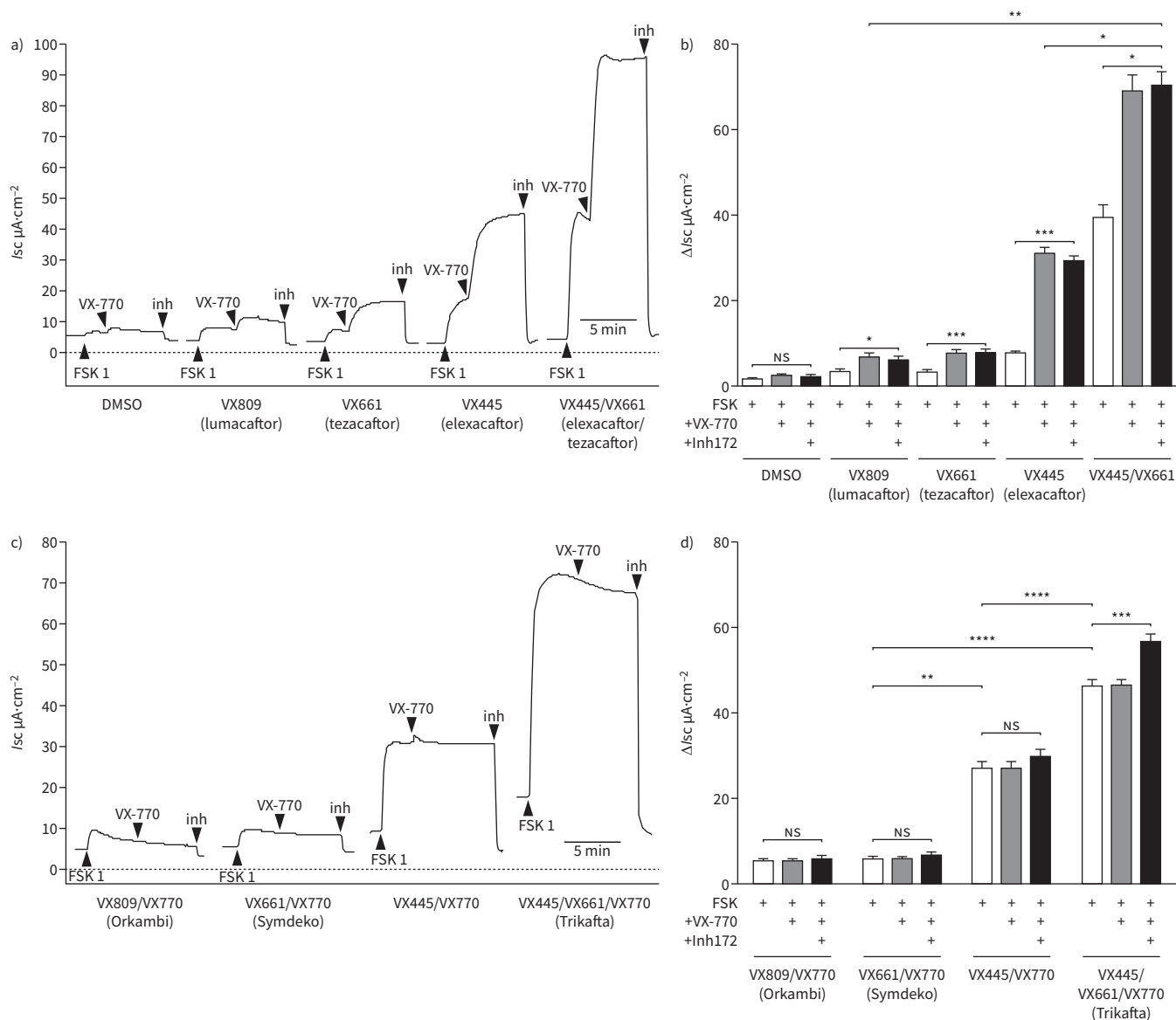


**FIGURE 2** Rescue of F508del short-circuit currents ( $I_{sc}$ ) by various correctors in CFBE cells expressing F508del-CFTR (cystic fibrosis transmembrane conductance regulator). Original tracings of  $I_{sc}$  as function of time for CFBE F508del cells incubated for 24 h with the corrector indicated below each plot a) without or c) with VX770. In a), dimethyl sulfoxide (DMSO) was used as control. The  $I_{sc}$  CFTR current was stimulated by forskolin at 1  $\mu M$  (FSK 1) and then 1  $\mu M$  VX770 and finally inhibited by 10  $\mu M$  CFTRinh172. b, d) Mean  $\pm$  SEM of  $\Delta I_{sc}$  for each condition illustrated in a) ( $n=5-14$ ) and c) ( $n=17$ ). NS: nonsignificant; \*:  $p<0.05$ , \*\*:  $p<0.01$ , \*\*\*:  $p<0.001$ , \*\*\*\*:  $p<0.0001$ .

inhibition of  $I_{sc}$  as shown figure 2b. The amplitude of the current blocked by CFTRinh172 was not significantly different when compared to the maximum level of  $I_{sc}$  recorded after FSK+VX770.

#### VX770 is unable to potentiate the elexacaftor/tezacaftor/ivacaftor-corrected F508del current

Because the therapeutic preparation Trikafta/Kaftrio is composed of VX445+VX661+VX770 (3VX), we compared the responses of CFBE F508del-CFTR cells after treatment with the same correctors (as in figure 2a) supplemented with 1  $\mu M$  ivacaftor, to mimic Trikafta/Kaftrio. Figure 2c and d shows the stimulation of F508del-dependent  $I_{sc}$  in these experimental conditions. As for the results presented in figure 2a, we stimulated  $I_{sc}$  with FSK (1  $\mu M$ ) and then we added VX770 (1  $\mu M$ ). First, we found a significant difference ( $p<0.05$ ) between the FSK-dependent  $I_{sc}$  recorded with cells treated with 3VX ( $\Delta I_{sc_{3VX}}=46.4 \pm 1.4 \mu A \cdot cm^{-2}$ ,  $n=17$ ; figure 2d) compared to cells treated with 2VX ( $\Delta I_{sc_{2VX}}=40 \pm 2.8 \mu A \cdot cm^{-2}$ ,  $n=14$ ; figure 2b). Second, for all the correctors or combination of correctors tested, the FSK

activated *I*<sub>sc</sub> could not be further potentiated following the acute addition of VX770 (figure 2c). The maximum level of correction of 3VX ( $\Delta I_{sc_{3VX}}=46.6\pm 1.3 \mu A \cdot cm^{-2}$ ,  $n=17$ ) is significantly different ( $p<0.0001$ ) compared to 2VX ( $\Delta I_{sc_{2VX}}=69\pm 3.5 \mu A \cdot cm^{-2}$ ,  $n=14$ ) when cells were stimulated by FSK (1  $\mu M$ ) and acute-VX770 (1  $\mu M$ ) (figure 2b, d). We replicated these results with VX770 added acutely at various concentrations. To that end, we treated cells with either 3VX (supplementary figure S2a) or 2VX (supplementary figure S2b) and stimulated *I*<sub>sc</sub> with FSK (0.1  $\mu M$ ) and increasing concentrations of VX770 from 0.1 to 10  $\mu M$ . Whereas VX770 (0.1  $\mu M$ ) potently stimulated *I*<sub>sc</sub> of cells treated with 2VX as shown in figures 1b and 2a, it is not the case for cells treated with Trikafta as shown in figures 1c and 2c, even at high concentrations (supplementary figure S2a). VX770 is also able to stimulate *I*<sub>sc</sub> at lower concentrations of cells treated with 2VX (*i.e.* 0.01  $\mu M$ , data not shown), as shown previously [15].

We observed in HAE and CFBE F508del-CFTR cells that the effect of FSK to activate F508del-CFTR was more pronounced when VX770 was present in the treatment mixture. Indeed, our recordings of *I*<sub>sc</sub> always show that FSK (at 0.1 or 1  $\mu M$ ) stimulated *I*<sub>sc</sub> with a higher amplitude for cells treated with 3VX than by 2VX (figure 1, figure 2 and supplementary figure S2). We thus compared the effect of various concentrations of FSK on *I*<sub>sc</sub> for both conditions of treatment and found that at any FSK concentrations tested, the *I*<sub>sc</sub> amplitude was increased for 3VX-treated cells (supplementary figure S2c), *i.e.* most probably due to the presence of VX770. However, the half maximal effective concentration ( $EC_{50}$ ) values calculated for FSK (supplementary figure S2c) were comparable for cells treated with either 3VX (~153 nM) or 2VX (~183 nM), suggesting that FSK has a similar potency in stimulating *I*<sub>sc</sub>, but an increased efficacy when VX770 is present together with the correctors elexacaftor/tezacaftor. KEATING *et al.* [25] also showed that the *I*<sub>sc</sub> stimulated by FSK (10  $\mu M$ ) in human bronchial epithelial cells treated with Trikafta was increased compared to elexacaftor/tezacaftor treatment.

To confirm the successful functional rescue of F508del-CFTR by elexacaftor/tezacaftor/ivacaftor, as measured in Ussing experiments with human airway epithelial cells, we recorded F508del-CFTR whole-cell chloride currents in BHK cells stably expressing F508del-CFTR. F508del-CFTR BHK cells were treated with 3VX (Trikafta;  $n=15$ ) and DMSO ( $n=14$ ) as control. Supplementary figure S3 shows representative whole-cell current traces and corresponding current density/*V* curves from experiments at baseline, after addition of FSK (10  $\mu M$ )+GST (30  $\mu M$ ) and following addition of CFTRinh172 (10  $\mu M$ ). FSK+GST stimulated a chloride current only in 3VX-treated BHK cells (supplementary figure S3a and c). The current reversed at -40 mV, close to the theoretical reversal potential for a chloride current in our experimental conditions (see methods). Finally, adding CFTRinh172 (10  $\mu M$ ) inhibited the stimulated currents. These results show that the triple combination of Trikafta, elexacaftor/tezacaftor/ivacaftor, also restores F508del-CFTR function in the nonhuman BHK cell expressing F508del-CFTR.

#### ***F508del-CFTR maturation and apical staining are reduced by VX770***

To begin to understand why it seems to be better to add VX770 in a second time after elexacaftor/tezacaftor, we were interested by the impact of VX-770 on CFTR protein expression. In fact, it has been reported that ivacaftor destabilises F508del-CFTR [22, 23]. We thus performed Western blot and immunofluorescence analysis with CFBE F508del cells treated with correctors with or without ivacaftor. Figure 3 shows results of Western blot experiments ( $n=6$ ) on cells either cultured on an insert analysed after measuring *I*<sub>sc</sub> with Ussing experiments (figure 3a) or on a plastic dish (figure 3b). The amount of mature F508del proteins (band C) was significantly increased for CFBE F508del-CFTR cells treated with tezacaftor, elexacaftor, elexacaftor/tezacaftor and elexacaftor/tezacaftor/ivacaftor compared to nontreated cells (figure 3c). In addition, the amount of band C of F508del-CFTR was significantly decreased in cells treated with 3VX compared with cells treated with 2VX (figure 3c). Comparable results were obtained for BHK cells expressing F508del-CFTR. The level of mature F508del proteins (band C) was also increased with 2VX or 3VX treatment (supplementary figure S3d).

Destabilisation of F508del-CFTR by VX770 was also studied by F508del-CFTR immunostaining. Figure 4 presents representative confocal images showing levels of CFTR immunofluorescent staining after 24-h incubation with DMSO, elexacaftor/tezacaftor (2VX) and elexacaftor/tezacaftor/ivacaftor (3VX) (figure 4a) and representative Z section of 3D confocal images showing apical localisation of CFTR staining along thickness of 3D culture in these experimental conditions (figure 4b). We quantified the mean intensity of fluorescence measured from Z maximum intensity projection images (figure 4c) and show the reduced intensity of CFTR immunofluorescent staining after 3VX compared to 2VX ( $p<0.001$ ). Although we cannot strictly correlate our results obtained by Western blot, Ussing chamber and immunolocalisation, these observations qualitatively confirmed that ivacaftor reduces the correction efficacy of Trikafta as shown earlier by others for VX809 (lumacaftor) and VX661 (tezacaftor) [22, 23].

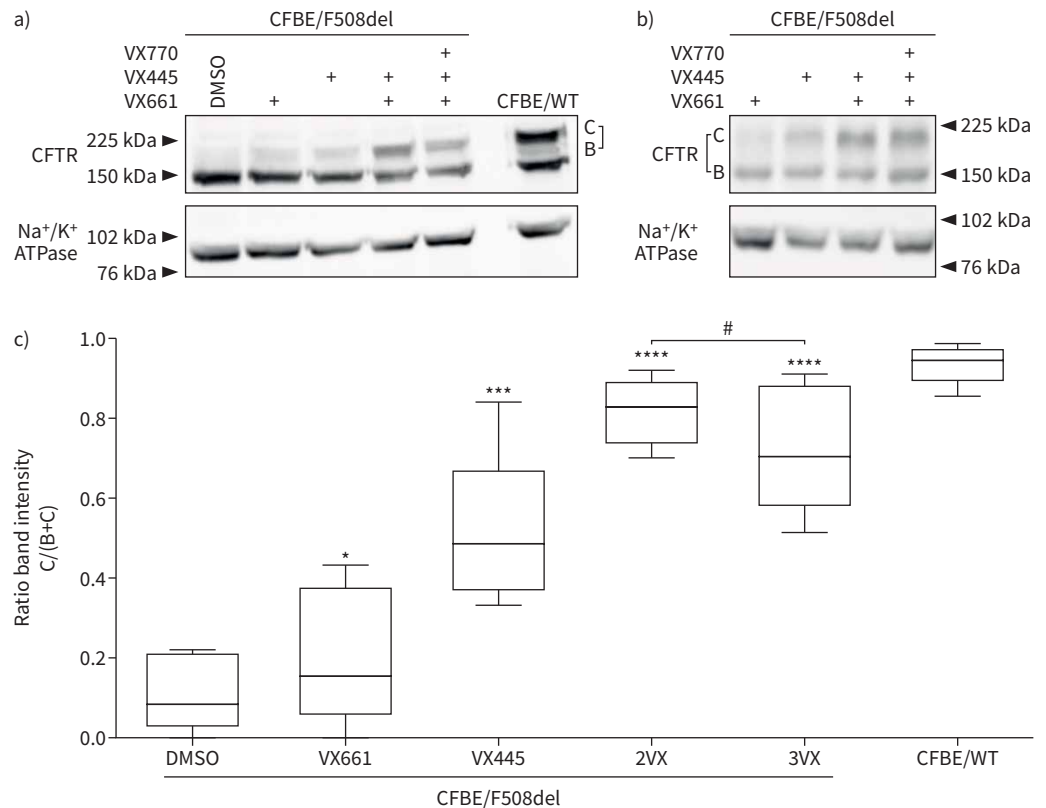


**FIGURE 3** Immunoblots of F508del following treatments with cystic fibrosis transmembrane conductance regulator (CFTR) correctors. **a)** CFTR expression of the total protein fraction of CFBE F508del cells after 24-h incubation with VX661 (18  $\mu$ M), VX445 (3  $\mu$ M) and VX770 (1  $\mu$ M) or dimethyl sulfoxide (DMSO) control and of CFBE wild-type (WT) cells grown on inserts (representative blot of six independent experiments). Equal protein loading was controlled *via* Na<sup>+</sup>/K<sup>+</sup> ATPase detection. **b)** CFTR expression of the total protein fraction from CFBE F508del cells, grown on a plastic dish, after 24-h incubation with VX661 (18  $\mu$ M), VX445 (3  $\mu$ M) and VX770 (1  $\mu$ M) (representative blot of two independent experiments). Equal protein loading was controlled *via* Na<sup>+</sup>/K<sup>+</sup> ATPase detection. **c)** Results of densitometric analysis of blots illustrated in **a)** expressed as ratio of mature form C to the sum of forms B+C from CFBE F508del and CFBE wild-type cells (n=6). Results are presented as mean $\pm$ SEM. Statistics are *versus* DMSO control: \*, p<0.05, \*\*\*, p<0.001, \*\*\*\*, p<0.0001; or *versus* 2VX treatment: #: p<0.05.

### The basal *I*<sub>sc</sub> current measured before stimulation as a marker of F508del rescue

During analysis of the Ussing chamber recordings after the various treatments shown in figures 1 and 2, we observed that the basal level of *I*<sub>sc</sub> was dependent on the nature of the correction. The value of basal *I*<sub>sc</sub> was quantified after amiloride and before stimulation by FSK. In particular with the triple combination elexacaftor/tezacaftor/ivacaftor, we systematically recorded a higher basal *I*<sub>sc</sub> compared to other treatments (figure 1d and figure 2c). With CFBE F508del cells, we determined the basal *I*<sub>sc</sub> for all experiments and reported the results in figure 5. For cells treated with only one corrector, either lumacaftor (VX809, n=7), tezacaftor (VX661, n=10) or elexacaftor (VX445, n=14), the basal *I*<sub>sc</sub> was not significantly different compared to DMSO (n=5) and nontreated cells (n=15; figure 5a). The value of basal *I*<sub>sc</sub> was also similar for cells treated with one corrector associated to the potentiator VX770 that is either the components of Orkambi (*i.e.* lumacaftor/ivacaftor; *I*<sub>sc</sub>=6.4 $\pm$ 0.8  $\mu$ A $\cdot$ cm<sup>-2</sup>, n=6) or of Symdeko (*i.e.* tezacaftor/ivacaftor; *I*<sub>sc</sub><sub>basal</sub>=5 $\pm$ 0.5  $\mu$ A $\cdot$ cm<sup>-2</sup>, n=10; figure 5b). However, the basal *I*<sub>sc</sub> value was significantly increased if ivacaftor is associated to elexacaftor treatment (*I*<sub>sc</sub><sub>basal</sub>=12 $\pm$ 1.1  $\mu$ A $\cdot$ cm<sup>-2</sup>, n=10; figure 5b). In the case of the association of two correctors, the basal *I*<sub>sc</sub> with elexacaftor/tezacaftor was *I*<sub>sc</sub><sub>basal</sub>=8 $\pm$ 0.5  $\mu$ A $\cdot$ cm<sup>-2</sup> (n=48) and increases to *I*<sub>sc</sub><sub>basal</sub>=17 $\pm$ 0.4  $\mu$ A $\cdot$ cm<sup>-2</sup> if it is associated with the potentiator VX770 (n=68; figure 5c). The basal *I*<sub>sc</sub> was comparable when tezacaftor was substituted by lumacaftor (*I*<sub>sc</sub><sub>basal</sub>=19 $\pm$ 1.6  $\mu$ A $\cdot$ cm<sup>-2</sup>, n=4; figure 5c). The substitution of VX661 by VX809 in the triple combination of Trikafta, neither modifies the FSK-stimulated *I*<sub>sc</sub> (VX809:  $\Delta$ *I*<sub>sc</sub>=49 $\pm$ 2.7  $\mu$ A $\cdot$ cm<sup>-2</sup>, n=4, 1  $\mu$ M FSK) nor the CFTRinh172-dependent *I*<sub>sc</sub> (VX809:  $\Delta$ *I*<sub>sc</sub>=50 $\pm$ 1.1  $\mu$ A $\cdot$ cm<sup>-2</sup>, n=4). Then, to confirm that the basal current was due to CFTR activity, we added the CFTR inhibitor directly on the basal current. An example is

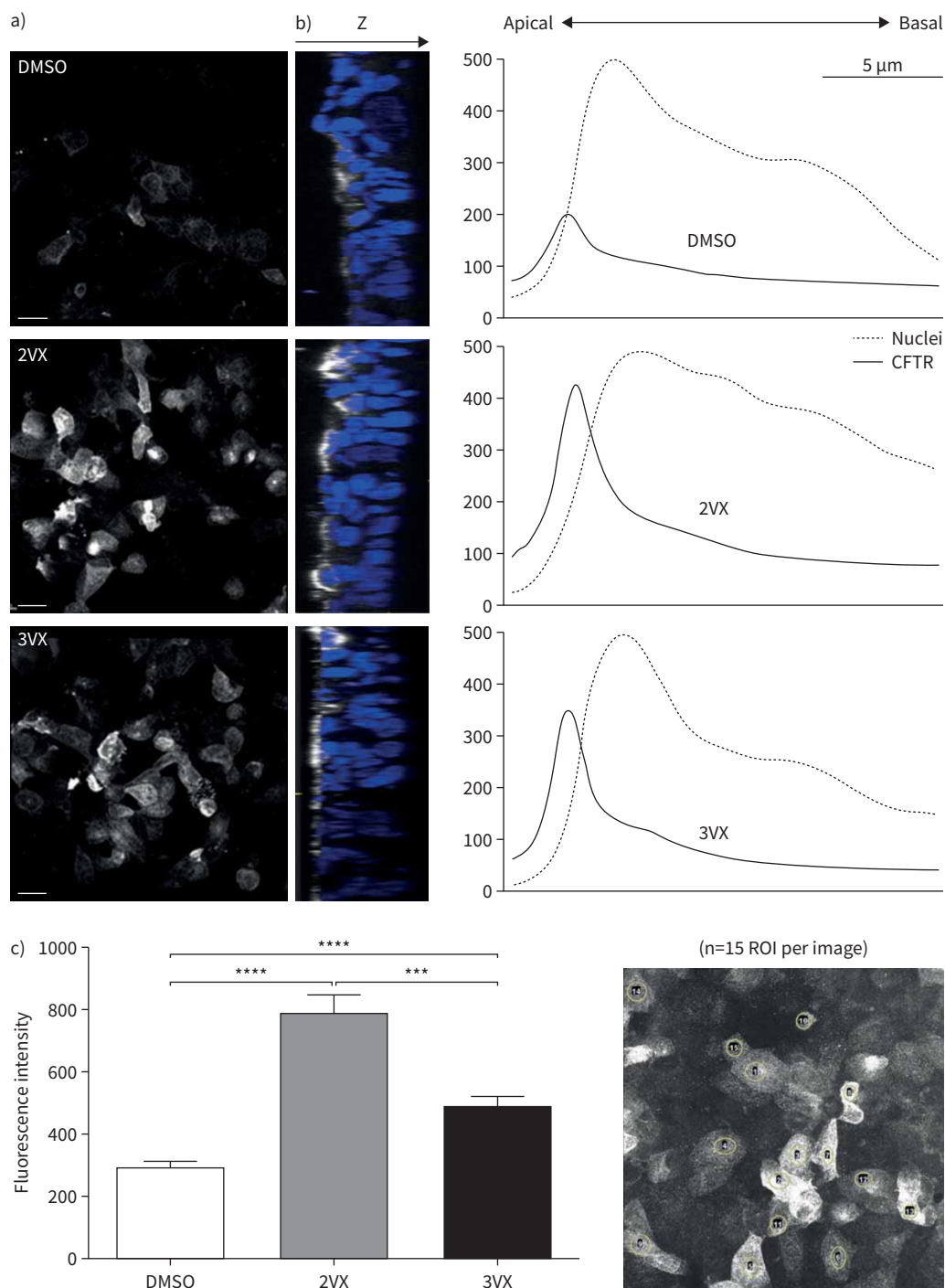


**FIGURE 4** Effect of correctors on cystic fibrosis transmembrane conductance regulator (CFTR) membrane localisation on polarised cultured of CFBE F508del epithelial cells. **a)** Representative confocal images showing level of F508del-CFTR immunofluorescent staining after 24-h incubation with dimethyl sulfoxide (DMSO), ellexacaftor/tezacaftor (2VX) or ellexacaftor/tezacaftor/ivacaftor (3VX). Images are maximum intensity projection of Z-stack. Scale bar=20 μm. **b)** Representative Z section of three-dimensional (3D) confocal images showing apical localisation of CFTR staining along thickness of 3D culture (two to three cell layers were revealed with diamidino-phenyl-indole (DAPI) staining). Graphs represent localisation of CFTR (revealed with AF647-coupled antibody) and nuclei (stained with DAPI) from apical to basal Z position. For each experimental condition, curves were obtained from fluorescence mean intensity values calculated along Z series (0.2 μm Z step, five images per condition, 15 regions of interest (ROI) per image). **c)** Mean intensity of fluorescence measured from Z maximum intensity projection images. A minimum 15 ROI were defined on the enhanced contrast display image. Results are presented as mean±SEM. Statistical analysis was performed by multiple comparisons using Mann-Whitney tests. \*\*\*: p<0.001, \*\*\*\*: p<0.0001.

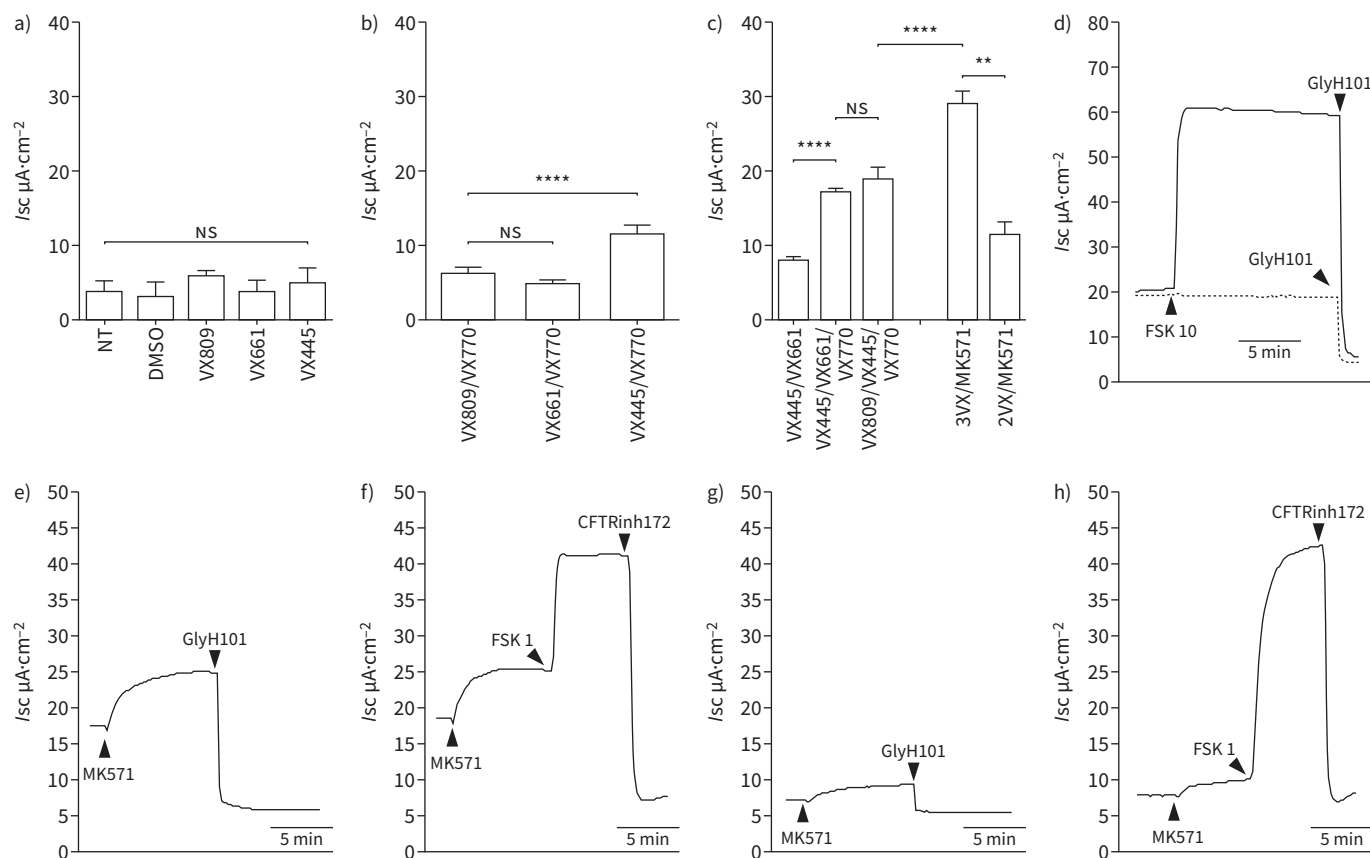


**FIGURE 5** Determination of the basal short-circuit currents ( $I_{sc}$ ). a–c) Averaged basal  $I_{sc}$  currents before forskolin (FSK) stimulation for each treatment condition on CFBE F508del cells. Results are presented as mean  $\pm$  SEM. d) Two superimposed original tracings showing  $I_{sc}$  for CFBE F508del cells incubated with ellexacaftor/tezacaftor/ivacaftor and stimulated with FSK (10  $\mu M$ ) or not. The CFTR (cystic fibrosis transmembrane conductance regulator) inhibitor GlyH-101 (15  $\mu M$ ) was used to block  $I_{sc}$ . Original tracings showing  $I_{sc}$  with CFBE F508del cells incubated with e, f) Trikafta and g, h) ellexacaftor/tezacaftor.  $I_{sc}$  was stimulated by the multidrug resistance protein 4 inhibitor MK571 (20  $\mu M$ ). FSK was used at 1  $\mu M$  in f) and h). To block CFTR-dependent  $I_{sc}$  we used either GlyH-101 (15  $\mu M$ , e) and g) or CFTRinh172 (10  $\mu M$ , f) and h)). Arrows indicate when agents were added. ns: nonsignificant; \*\*:  $p < 0.01$ , \*\*\*\*:  $p < 0.0001$ .

shown in figure 5d. In these paired experiments we treated cells by ellexacaftor/tezacaftor/ivacaftor and added GlyH101 (15  $\mu M$ ) with or without FSK (10  $\mu M$ ) as indicated on the tracings. After GlyH101, both inhibited currents reached a comparable level. Thus, the inhibited  $I_{sc}$  current represents the sum of the basal activity of CFTR plus the FSK-activated CFTR activity. Therefore, treating cells with Trikafta, most probably due to the presence of the CFTR potentiator ivacaftor, results in the basal cAMP activation of F508del-CFTR in the absence of any exogenous addition of cAMP agonists. To further study this, in the next experiments we used MK571 an inhibitor of the multidrug resistance protein 4 (MRP4/ABCC4) [37] which is expressed in airway epithelial cells [38, 39]. Inhibition of MRP4 by MK571 was shown to prevent cAMP efflux within cellular microdomains containing MRP4 and CFTR, thereby augmenting phosphorylation of CFTR [37–39]. With CFBE F508del cells treated with ellexacaftor/tezacaftor/ivacaftor (figure 5e, f) and ellexacaftor/tezacaftor (figure 5g, h), a pre-incubation with MK571 (20  $\mu M$ ) for 20 min in the apical chamber induced a further increase of basal  $I_{sc}$  ( $I_{sc_{basal}} = 29 \pm 1.6 \mu A \cdot cm^{-2}$  and  $11 \pm 1.7 \mu A \cdot cm^{-2}$ , respectively; figure 5c). Representative recordings are shown in figures 5e–h. Addition of the CFTR inhibitors GlyH101 (15  $\mu M$ ) or CFTRinh172 (10  $\mu M$ ) inhibited  $I_{sc}$  in absence of additional stimulation (figure 5e, g) or after 1  $\mu M$  FSK (figure 5f, h). In addition, we observed that the effect of MK571 was significantly reduced ( $p < 0.01$ ) in cells treated with ellexacaftor/tezacaftor compared to cells treated with ellexacaftor/tezacaftor/ivacaftor (figure 5c).

#### Potentiation of Trikafta-corrected F508del-CFTR function

A striking difference observed in both HAE (figure 1) or CFBE F508del cells (figure 2) treated with ellexacaftor/tezacaftor/ivacaftor or by only the two correctors ellexacaftor/tezacaftor (i.e. without ivacaftor) is that adding

VX770 cannot further increase *I*<sub>sc</sub>. Of note, the prescription of Trikafta to CF patients consists of a first tablet with the triple combination elexacaftor/tezacaftor/ivacaftor and a second tablet with only ivacaftor. Although our *in vitro* analysis of the effect of the components of Trikafta cannot be strictly compared to an *in vivo* exposure of CF patients to Trikafta, we conducted additional experiments to study this difference in more details. To that end, we used elexacaftor/tezacaftor/ivacaftor-treated cells stimulated by 0.1 μM FSK (corresponding to the calculated EC<sub>50</sub> value as shown; supplementary figure S2c). Acute addition of VX770 (1 μM) before (figure 6a) or after FSK at different concentrations (figure 6b, c) failed to increase *I*<sub>sc</sub>. To evaluate whether the amplitude of the current reached after FSK+VX770 was maximal, we added 1 μM FSK (corresponding to the saturating concentration; supplementary figure S2c) after VX770. The addition of 1 μM FSK after VX770 increased *I*<sub>sc</sub> (figure 6a–c), which was inhibited by CFTRinh172. Then, we evaluated the effect of VX770 on cells treated with elexacaftor/tezacaftor. As expected, VX770 (1 μM) was able to stimulate *I*<sub>sc</sub> before (figure 6d) or after FSK (figure 6e, f) and was inhibited by CFTRinh172. However, VX770-dependent *I*<sub>sc</sub> was not maximal because it could be further potentiated by FSK (0.1–1 μM) as shown in figure 6d–f. The *I*<sub>sc</sub> presented in figures 6a and 6d are summarised in figure 6g. Figure 6h shows results when high concentration of FSK (10 μM) was added before adding VX770 (1 μM) for cells treated with either 3VX or 2VX.

Our next question was to determine whether a different potentiator, instead of VX770, would be able to potentiate FSK-activated *I*<sub>sc</sub> in Trikafta-treated cells. We thus conducted experiments with the two potentiators, genistein [31] and Cact-A1 [32] and compared their effects with cells treated with either elexacaftor/tezacaftor/ivacaftor (figure 7a) or elexacaftor/tezacaftor (figure 7b). We first used a low concentration of FSK (0.01 μM) to pre-stimulate *I*<sub>sc</sub> and then added genistein (30 μM) or Cact-A1 (30 μM) and finally added saturating FSK (1 μM). In contrast to VX770, both potentiators significantly potentiated the FSK-dependent *I*<sub>sc</sub> (figure 7a, b). However, the effect of saturating concentration of FSK was very small compared to the experiments using VX770 (figure 6c, f and figure 7a, b). Since VX770 binds within the transmembrane region of CFTR protein [40], it might prevent the action of different potentiators. Thus, we recorded *I*<sub>sc</sub> with CFBE F508del cells treated with either elexacaftor/tezacaftor/ivacaftor (figure 8a, c) or elexacaftor/tezacaftor (figure 8b, c) stimulated by genistein after VX770. We obtained comparable results with F508del-HAE cells treated with either elexacaftor/tezacaftor/ivacaftor (figure 8d, f) or elexacaftor/tezacaftor (figure 8e, f) stimulated by genistein after VX770. In both cell models, these results show that genistein is able to potentiate *I*<sub>sc</sub> despite the presence of VX770.

## Discussion

The novel medicament for CF patients, Trikafta/Kaftrio (Vertex Pharmaceuticals, USA), is composed of two folding correctors, elexacaftor and tezacaftor, and one gating potentiator, ivacaftor. The results of phase 3 clinical trials demonstrated a significant gain in lung function with Trikafta as compared to Orkambi and Symdeko (table 1; www.cff.org) [25–27]. Trikafta is indicated for CF patients aged ≥12 years who have at least one F508del mutation, or at least one other mutation in the CF gene that is responsive to Trikafta (*i.e.* 177 other approved mutations), regardless of their second mutation type (www.cff.org). Although the molecular mechanism of action of these modulators remains unknown, Trikafta might help F508del-CFTR to fold properly to be relocated to the apical plasma membrane of epithelial cells instead of being addressed to the intracellular degradation pathway. Then, the corrected F508del-defective CFTR protein functions more efficiently at the apical membrane of airway epithelial cells [25–29]. In a recent study, VEIT *et al.* [28] showed that VX445 synergistically restores F508del-CFTR processing in combination with correctors of type I (such as VX661, VX809, ABBV-2222 and FDL169) or II (the compound 3151; [41]). These correctors target the NBD1-MSD interface and NBD2, respectively. These authors proposed that VX445 is a type III corrector stabilising NBD1 [28, 41]. This is consistent with our results showing synergy between VX445 and VX661 and with results from experiments in which we substituted VX661 by VX809 (two type I correctors) in the triple combination of Trikafta, and observed no significant differences in the values of Δ*I*<sub>sc</sub>. Another recent investigation on double corrector treatment [42] showed that VX445 elicits a large rescue of F508del-CFTR function, as we observed here. However, after analysis of ubiquitylation, resistance to thermoaggregation, protein half-life and subcellular localisation authors concluded that VX445 plus a type I corrector (VX661 or VX809) did not fully normalise F508del-CFTR behaviour.

We have explored in that study the effect of the three components of Trikafta (*i.e.* elexacaftor/tezacaftor/ivacaftor) either alone or in combination and found that in the absence of the potentiator ivacaftor, the order of potency to rescue F508del-CFTR function was lumacaftor ~ tezacaftor << elexacaftor << elexacaftor/tezacaftor; the two folding correctors elexacaftor and tezacaftor acting synergistically [25, 28]. In the presence of the potentiator ivacaftor, we found differences in the order of potency for the ability to rescue F508del function as determined by the amplitude of the FSK-dependent *I*<sub>sc</sub>. In that case, Trikafta was the most potent treatment: Orkambi ~ Symdeko << elexacaftor/ivacaftor << Trikafta. Conversely, we found that the order of potency to rescue the mature form of F508del proteins (form C) was tezacaftor <<

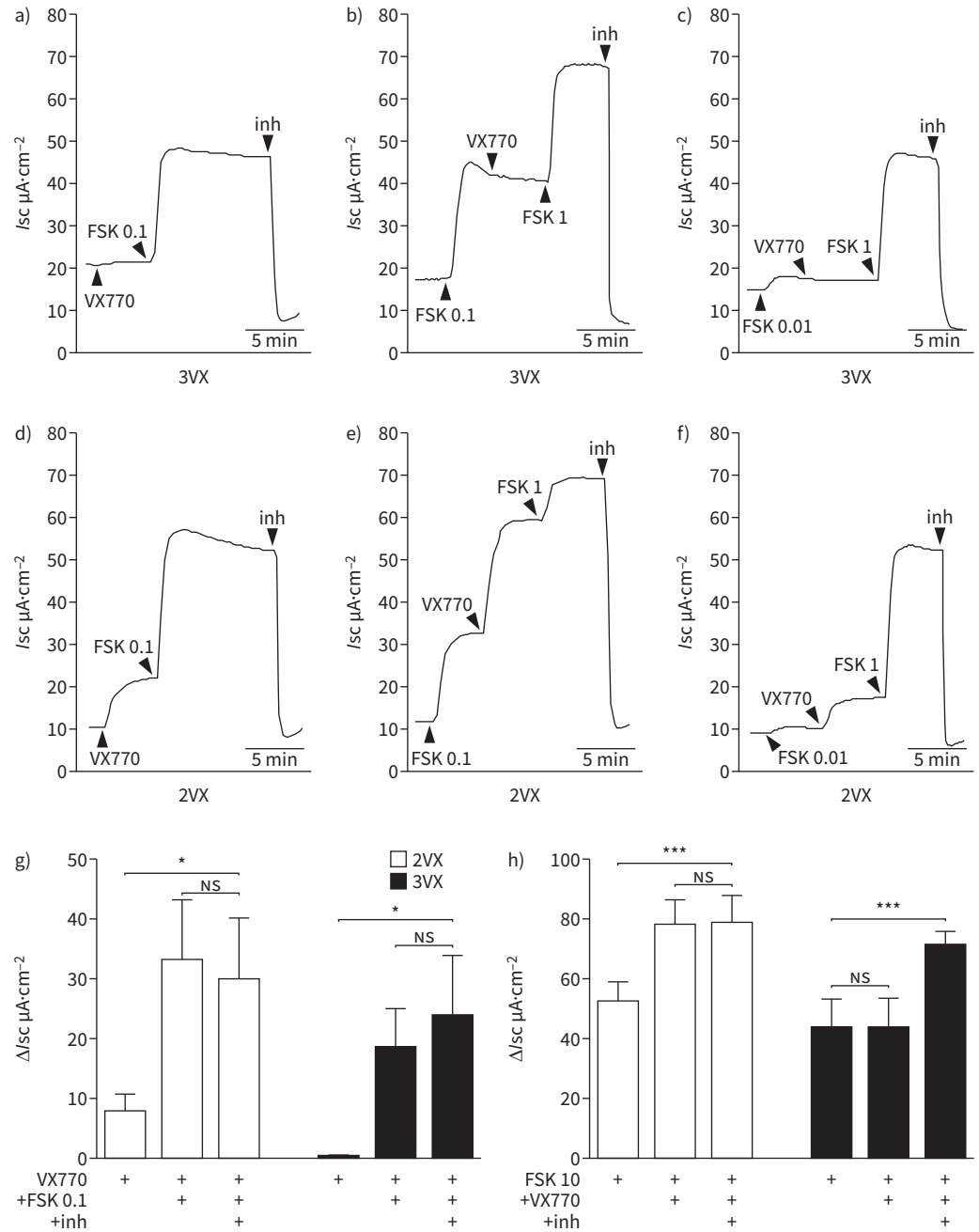


**FIGURE 6** Acute VX770 stimulates F508del short-circuit currents (*I*<sub>sc</sub>) in elexacaftor/tezacaftor- but not in Trikafta-treated cells. Original tracings showing *I*<sub>sc</sub> for CFBE F508del cells treated with a-c) elexacaftor/tezacaftor/ivacaftor or d-f) elexacaftor/tezacaftor. The *I*<sub>sc</sub> current was stimulated by different combinations of VX770 (1  $\mu$ M) and forskolin (FSK; 0.01, 0.1 or 1  $\mu$ M). The concentrations are indicated on each plot. Inh: CFTR (cystic fibrosis transmembrane conductance regulator)inh172 (10  $\mu$ M). **g, h** Mean  $\pm$ SEM of  $\Delta I_{sc}$  as indicated under each bar histogram (n=4-8). NS: nonsignificant; \*, p<0.05, \*\*\*, p<0.001.

elexacaftor ~ elexacaftor/tezacaftor/ivacaftor < elexacaftor/tezacaftor. A similar result was reported by KEATING *et al.* [25].

However, for the triple-combination Trikafta (this study and [25, 28]), as for the double combinations Orkambi and Symdeko [22, 23], the gating potentiator ivacaftor reduced the correction efficacy of these treatments as observed for F508del-CFTR localisation, maturation and function in airway epithelial cells. As reported earlier with lumacaftor and tezacaftor [22-24], this effect is due to the progressive loss of

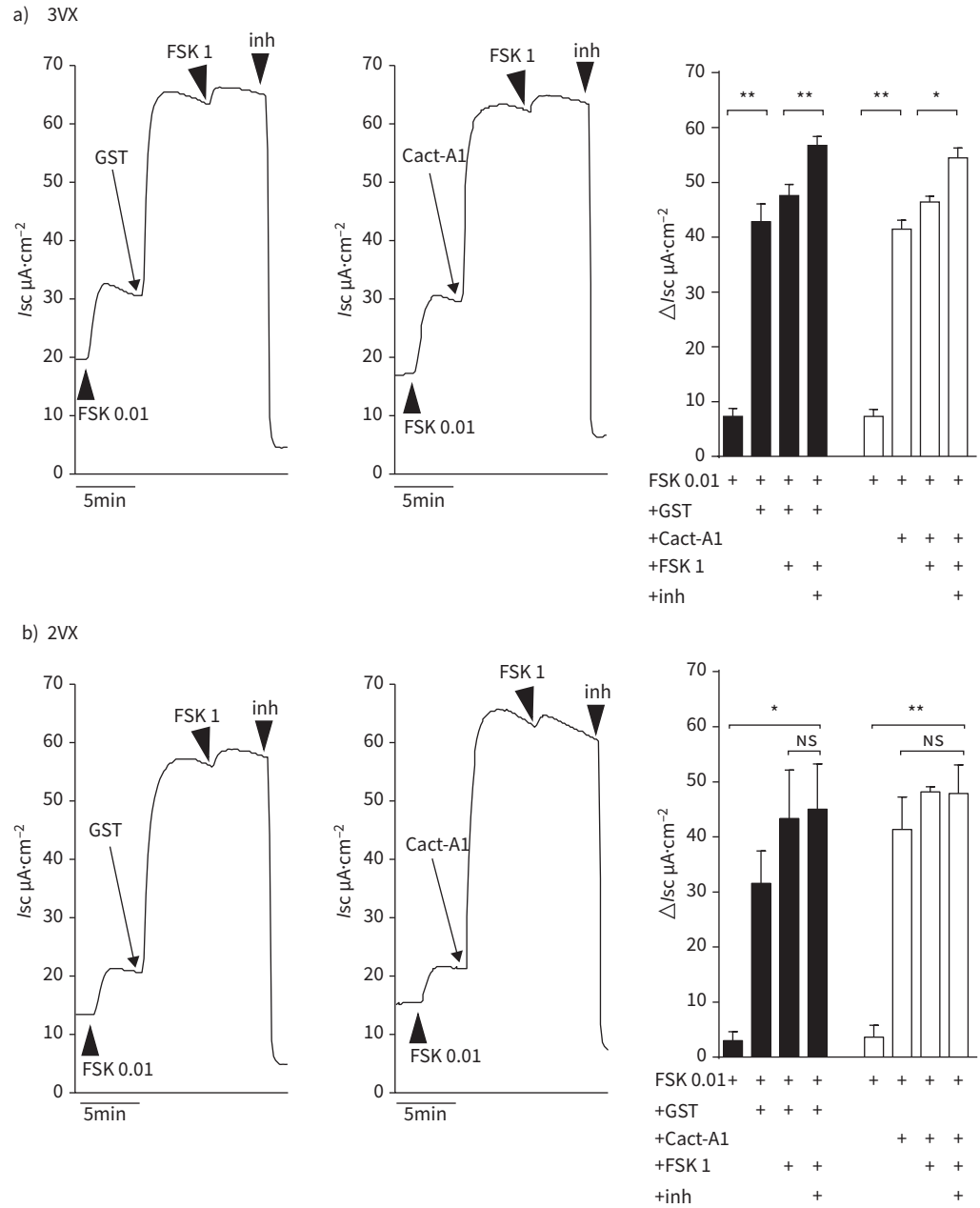


**FIGURE 7** Genistein and Cact-A1 stimulate F508del short-circuit currents (*I*<sub>sc</sub>) in elixacaftor/tezacaftor- and in Trikafta-treated cells. Original tracings showing *I*<sub>sc</sub> for CFBE F508del cells treated with a) elixacaftor/tezacaftor/ivacaftor (3VX) or b) elixacaftor/tezacaftor (2VX). *I*<sub>sc</sub> currents stimulated by different combinations of forskolin (FSK), genistein (GST; 30 µM) and Cact-A1 (30 µM). Inh: CFTR (cystic fibrosis transmembrane conductance regulator)inh172 (10 µM). In a) (n=5) and b) (n=4), the histograms on the right show the mean±SEM of Δ*I*<sub>sc</sub>. NS: no significant difference; \*: p<0.05, \*\*: p<0.01.

CFTR at the plasma membrane following its activation. An effect that might also be related to the lipophilicity of ivacaftor at the origin of nonspecific effects on the lipid bilayer [43]. This membrane effect may account for the destabilising effect of ivacaftor on lumacaftor-rescued F508del-CFTR as recently shown [43]. Our Western blot and immunolocalisation studies of F508del proteins are in good agreement with these observations and therefore confirmed that ivacaftor has also a destabilising effect on F508del rescued by Trikafta, as shown [25, 28].

A comparison of the basal *I*<sub>sc</sub> suggests that the inhibited *I*<sub>sc</sub> current represents the sum of the basal activity of CFTR plus the FSK/potentiator-activated CFTR activity (*i.e.* supplementary figure S1c a+b+c).

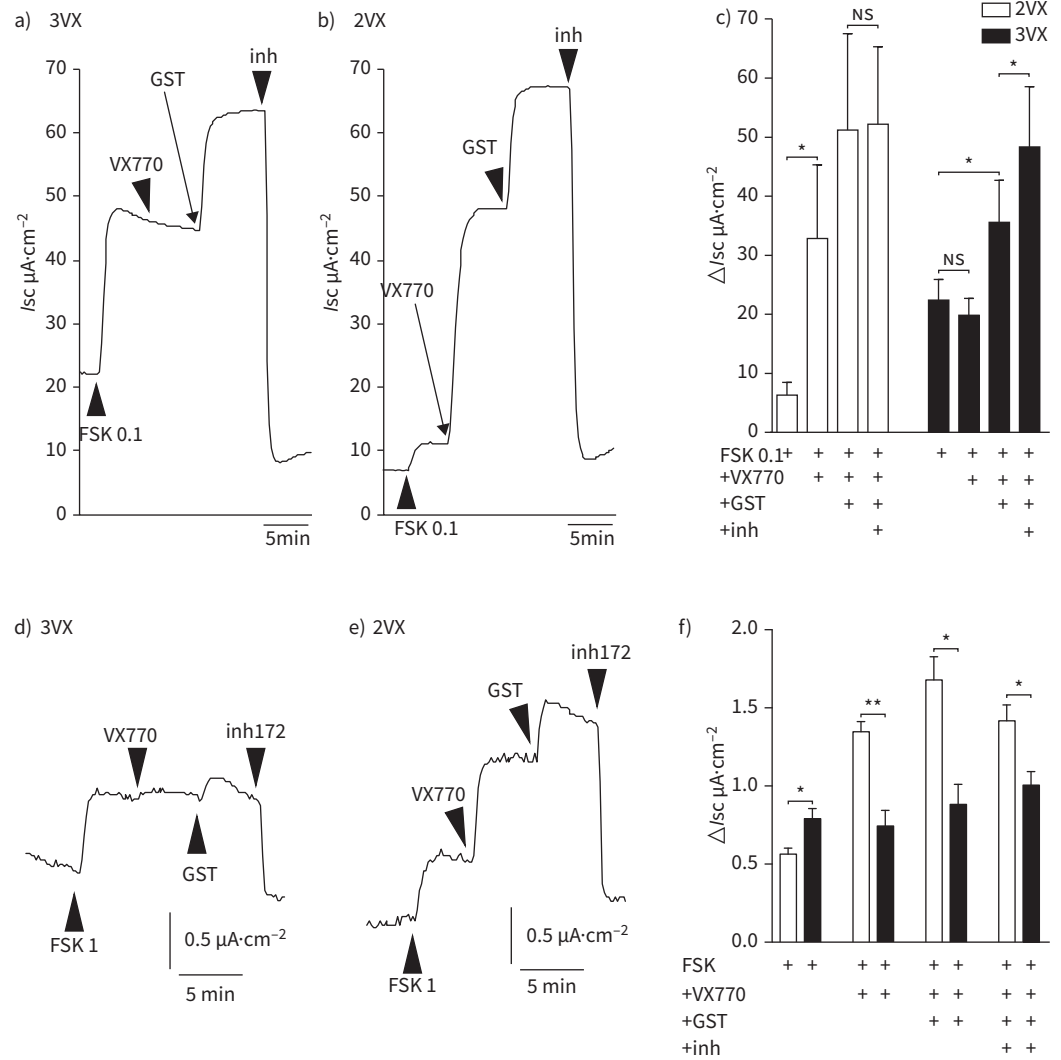


**FIGURE 8** Genistein added after VX770 stimulates F508del short-circuit currents (*I*<sub>sc</sub>) in ellexacaftor/tezacaftor- and Trikafta-treated cells. Original tracings showing *I*<sub>sc</sub> for CFBE F508del cells treated with **a)** ellexacaftor/tezacaftor/ivacaftor (3VX) and **b)** ellexacaftor/tezacaftor (2VX). **c)** Mean ± SEM of Δ*I*<sub>sc</sub> (n=4-5) in response to forskolin (FSK; 0.1 μM), VX770 (1 μM) and genistein (GST; 30 μM). Inh: CFTR (cystic fibrosis transmembrane conductance regulator)CFTRinh172 (10 μM) as indicated below each bar histogram. Original tracings showing *I*<sub>sc</sub> for HAE F508del cells treated with **d)** ellexacaftor/tezacaftor/ivacaftor and **e)** ellexacaftor/tezacaftor. **f)** Mean ± SEM of Δ*I*<sub>sc</sub> (n=3) in response to FSK (1 μM), VX770 (1 μM) and genistein (GST; 30 μM) as indicated below each bar histogram. NS: nonsignificant; \*: p<0.05, \*\*: p<0.01.

Thus, we believe that with Trikafta, the basal *I*<sub>sc</sub> reflects the fact that F508del-CFTR is not only resident (due to the synergic correcting action of ellexacaftor/tezacaftor), but also functional at the plasma membrane of cells (due to the binding of ivacaftor to F508del-CFTR and opening of the channels) under the control of an endogenous cAMP pathway. A raise of the basal and FSK-mediated *I*<sub>sc</sub> by MK-571 in ellexacaftor/tezacaftor/ivacaftor- or ellexacaftor/tezacaftor-treated cells could occur through induction of local elevations in cytosolic cAMP as suggested by the description of the spatiotemporal coupling between the cAMP transporter MRP4 and CFTR activity in intestinal [37] and airway cells [38, 39]. Therefore, we propose here that the basal *I*<sub>sc</sub>, a value generally neglected, could represent a marker of the level of correction of functional F508del-CFTR and could serve as a readthrough to identify synergistic combinations of F508del-CFTR modulators. Our results are in agreement with those of KEATING *et al.* [25], showing that the *I*<sub>sc</sub> stimulated by FSK in human airway epithelial cells treated with Trikafta was increased compared to a treatment by ellexacaftor/tezacaftor.

We believe that the level of stimulation of CFTR-dependent *I*<sub>sc</sub> is underestimated when ivacaftor is used as potentiator. Despite the fact that ivacaftor was very potent to acutely potentiate the rescued F508del-CFTR-dependent *I*<sub>sc</sub> when cells were treated with elxacaftor/tezacaftor, the potentiator was unable to activate CFTR-*I*<sub>sc</sub> in Trikafta-treated cells. At least two studies might explain our results. First, recent evidence from experiments of cryoelectron microscopy showed structure of human CFTR in complex with the two potentiators ivacaftor and GLPG1837 binding to the same site within the transmembrane region of CFTR [40]. Therefore, a direct binding of ivacaftor to F508del might explain why, after 24 h incubation, the acute addition of ivacaftor was unable to stimulate CFTR current, simply because the binding sites are still occupied. This was not the case for genistein and Cact-A1 which are still able to stimulate the rescued F508del current above the level achieved by FSK and despite the presence of ivacaftor (chronic or acute). The most plausible reason is that ivacaftor and genistein do not compete for the same binding site. Indeed, genistein has been shown to interact with nucleotide-binding domains (although no binding has been firmly shown) [44, 45], but not with the transmembrane region of CFTR where ivacaftor binds [40]. Unfortunately, genistein has no clinical benefit on some CFTR variants [46] and therefore cannot replace ivacaftor. Secondly, it has been shown that ivacaftor accumulates in CF-HBE cells to a much greater extent than either lumacaftor or tezacaftor, remaining persistently elevated even after 14 days of washout. CFTR activity peaked at 7 days of treatment, but diminished with further ivacaftor accumulation, although remained it above baseline even after washout [47].

In conclusion, our study confirms the efficacy of the components of Trikafta to rescue a mature and functional form of F508del-CFTR at the apical plasma membrane of human airway epithelial cells. In addition, we show that ivacaftor has still a destabilising effect on rescued-F508del and that despite the potency of ivacaftor, it was not able to further potentiate the function of Trikafta-rescued F508del-CFTR. This is important because ivacaftor also reduces the correction efficacy of lumacaftor [22, 23] and tezacaftor [23]. Our results also showed that ivacaftor does not preclude the use of another potentiator combined to Trikafta. Taken together with previous reports [13, 16, 22–24], our results thus suggest that we should be able to maximise the correcting effect of Trikafta by using a different potentiator.

Author contributions: F. Becq designed the experiments, analysed the data and contributed reagents/materials/analysis tools. F. Becq performed Ussing chamber experiments. F. Becq and T. Carrez performed and analysed patch-clamp experiments. A. Billet designed Nanion's protocols and established BHK stably expressing F508del-CFTR cells. S. Mirval carried out all cell cultures. S. Mirval and M. Lévêque performed and analysed Western blot experiments. A. Cantereau performed and analysed confocal imaging and immunolocalisation experiments. C. Coraux and E. Sage collected and provided human airway epithelial cells. F. Becq, A. Cantereau and M. Lévêque wrote and edited the manuscript.

Conflict of interest: The authors declare that they have no conflict of interest.

Support statement: This study was supported by Vaincre La Mucoviscidose (RF20200502704). T. Carrez holds a thesis scholarship from ANRT and ManRos therapeutics *via* CIFRE. A. Billet was a recipient of post-doctoral fellowship from the CF Trust (SRC005). M. Lévêque holds a postdoctoral fellowship from Vaincre La Mucoviscidose (RF20200502704). This work has benefited from the facilities and expertise of ImageUP platform (University of Poitiers). Funding information for this article has been deposited with the Crossref Funder Registry.

## References

- 1 Rowe SM, Miller S, Sorscher EJ. Cystic fibrosis. *N Engl J Med* 2005; 352: 1992–2001.
- 2 Cheng SH, Gregory RJ, Marshall J, *et al.* Defective intracellular transport and processing of CFTR is the molecular basis of most cystic fibrosis. *Cell* 1990; 63: 827–834.
- 3 Denning GM, Ostedgaard LS, Welsh MJ. Abnormal localization of cystic fibrosis transmembrane conductance regulator in primary cultures of cystic fibrosis airway epithelia. *J Cell Biol* 1992; 118: 551–559.
- 4 Welsh MJ, Smith AE. Molecular mechanisms of CFTR chloride channel dysfunction in cystic fibrosis. *Cell* 1993; 73: 1251–1254.
- 5 Dalemans W, Barbry P, Champigny G, *et al.* Altered chloride ion channel kinetics associated with the  $\Delta$ F508 cystic fibrosis mutation. *Nature* 1991; 354: 526–528.
- 6 Lukacs GL, Chang XB, Bear C, *et al.* The  $\Delta$ F508 mutation decreases the stability of cystic fibrosis transmembrane conductance regulator in the plasma membrane. Determination of functional half-lives on transfected cells. *J Biol Chem* 1993; 268: 21592–21598.
- 7 Okiyoneda T, Barrière H, Bagdány M, *et al.* Peripheral protein quality control removes unfolded CFTR from the plasma membrane. *Science* 2010; 329: 805–810.

- 8 Liu X, Dawson DC. Cystic fibrosis transmembrane conductance regulator (CFTR) potentiators protect G551D but not  $\Delta$ F508 CFTR from thermal instability. *Biochemistry* 2014; 53: 5613–5618.
- 9 Wang W, Okeyo GO, Tao B, et al. Thermally unstable gating of the most common cystic fibrosis mutant channel ( $\Delta$ F508): “rescue” by suppressor mutations in nucleotide binding domain 1 and by constitutive mutations in the cytosolic loops. *J Biol Chem* 2011; 286: 41937–41948.
- 10 Cystic Fibrosis Foundation. Patient Registry: 2019 Annual Data Report. Bethesda, MD, Cystic Fibrosis Foundation, 2019.
- 11 Zolin A, Orenti A, Naehrlich L, et al. 2018 European Cystic Fibrosis Society Patient Registry Annual Data Report. Karup, European Cystic Fibrosis Society, 2020.
- 12 Veit G, Avramescu RG, Chiang AN, et al. From CFTR biology toward combinatorial pharmacotherapy: expanded classification of cystic fibrosis mutations. *Mol Biol Cell* 2016; 27: 424–433.
- 13 Okiyoneda T, Veit G, Dekkers JF, et al. Mechanism-based corrector combination restores  $\Delta$ F508-CFTR folding and function. *Nat Chem Biol* 2013; 9: 444–454.
- 14 Van Goor F, Hadida S, Grootenhuis PD, et al. Correction of the F508del-CFTR protein processing defect *in vitro* by the investigational drug VX-809. *Proc Natl Acad Sci USA* 2011; 108: 18843–18848.
- 15 Van Goor F, Hadida S, Grootenhuis PD, et al. Rescue of CF airway epithelial cell function *in vitro* by a CFTR potentiator, VX-770. *Proc Natl Acad Sci USA* 2009; 106: 18825–18830.
- 16 Dekkers JF, Van Mourik P, Vonk AM, et al. Potentiator synergy in rectal organoids carrying S1251N, G551D, or F508del CFTR mutations. *J Cyst Fibros* 2016; 15: 568–578.
- 17 Phuan PW, Tan J-A, Rivera AA, et al. Nanomolar-potency ‘co-potentiator’ therapy for cystic fibrosis caused by a defined subset of minimal function CFTR mutants. *Sci Rep* 2019; 9: 17640.
- 18 Wainwright CE, Elborn JS, Ramsey BW, et al. Lumacaftor-ivacaftor in patients with cystic fibrosis homozygous for Phe508del CFTR. *N Engl J Med* 2015; 373: 220–231.
- 19 Rehman A, Baloch NU, Janahi IA. Lumacaftor-ivacaftor in patients with cystic fibrosis homozygous for Phe508del CFTR. *N Engl J Med* 2015; 373: 1783.
- 20 Taylor-Cousar JL, Munck A, McKone EF, et al. Tezacaftor-ivacaftor in patients with cystic fibrosis homozygous for Phe508del. *N Engl J Med* 2017; 377: 2013–2023.
- 21 Rowe SM, Daines C, Ringhausen FC, et al. Tezacaftor-ivacaftor in residual-function heterozygotes with cystic fibrosis. *N Engl J Med* 2017; 377: 2024–2035.
- 22 Cholon DM, Quinney NL, Fulcher ML, et al. Potentiator ivacaftor abrogates pharmacological correction of  $\Delta$ F508 CFTR in cystic fibrosis. *Sci Transl Med* 2014; 6: 246ra96.
- 23 Veit G, Avramescu RG, Perdomo D, et al. Some gating potentiators, including VX-770, diminish  $\Delta$ F508-CFTR functional expression. *Sci Transl Med* 2014; 6: 246ra97.
- 24 Avramescu RG, Kai Y, Xu H, et al. Mutation-specific downregulation of CFTR2 variants by gating potentiators. *Hum Mol Genet* 2017; 26: 4873–4885.
- 25 Keating D, Marigowda G, Burr L, et al. VX-445-tezacaftor-ivacaftor in patients with cystic fibrosis and one or two Phe508del alleles. *N Engl J Med* 2018; 379: 1612–1620.
- 26 Heijerman HGM, McKone EF, Downey DG, et al. Efficacy and safety of the elexacaftor plus tezacaftor plus ivacaftor combination regimen in people with cystic fibrosis homozygous for the F508del mutation: a double-blind, randomised, phase 3 trial. *Lancet* 2019; 394: 1940–1948.
- 27 Middleton PG, Mall MA, Dřevínek P, et al. Elexacaftor-tezacaftor-ivacaftor for cystic fibrosis with a single phe508del allele. *N Engl J Med* 2019; 381: 1809–1819.
- 28 Veit G, Roldan A, Hancock MA, et al. Allosteric folding correction of F508del and rare CFTR mutants by elexacaftor-tezacaftor-ivacaftor (Trikafta) combination. *JCI Insight* 2020; 5: e139983.
- 29 Laselva O, Bartlett C, Gunawardena TNA, et al. Rescue of multiple class II CFTR mutations by elexacaftor+tezacaftor+ivacaftor mediated in part by the dual activities of elexacaftor as both corrector and potentiator. *Eur Respir J* 2021; 57: 2002774.
- 30 Froux L, Coraux C, Sage E, et al. The short-term consequences of F508del-CFTR thermal instability on CFTR-dependent transepithelial currents in human airway epithelial cells. *Sci Rep* 2019; 9: 13729.
- 31 Hwang T-C, Wang F, Yang IC-H, et al. Genistein potentiates wild-type and  $\Delta$ F508-CFTR channel activity. *Am J Physiol* 1997; 273: C988–C998.
- 32 Namkung W, Park J, Seo Y, et al. Novel amino-carbonitrile-pyrazole identified in a small molecule screen activates wild-type and  $\Delta$ F508 cystic fibrosis transmembrane conductance regulator in the absence of a cAMP agonist. *Mol Pharmacol* 2003; 84: 384–392.
- 33 Ma T, Thiagarajah JR, Yang H, et al. Thiazolidinone CFTR inhibitor identified by high-throughput screening blocks cholera toxin-induced intestinal fluid secretion. *J Clin Invest* 2002; 110: 1651–1658.
- 34 Muanprasat C, Sonawane ND, Salinas D, et al. Discovery of glycine hydrazide pore-occluding CFTR inhibitors: mechanism, structure-activity analysis, and *in vivo* efficacy. *J Gen Physiol* 2004; 124: 125–137.
- 35 Billet A, Froux L, Hanrahan JW, et al. Development of automated patch clamp technique to investigate CFTR chloride channel function. *Front Pharmacol* 2017; 8: 195.

- 36 Yu W, Chiaw PK, Bear CE. Probing conformational rescue induced by a chemical corrector of F508del-cystic fibrosis transmembrane conductance regulator (CFTR) mutant. *J Biol Chem* 2011; 286: 24714–24725.
- 37 Li C, Krishnamurthy PC, Penmatsa H, *et al.* Spatiotemporal coupling of cAMP transporter to CFTR chloride channel function in the gut epithelia. *Cell* 2007; 131: 940–951.
- 38 Schnúr A, Premchandrar A, Bagdany M, *et al.* Phosphorylation-dependent modulation of CFTR macromolecular signalling complex activity by cigarette smoke condensate in airway epithelia. *Sci Rep* 2019; 9: 12706.
- 39 Ahmadi S, Bozoky Z, Di Paola M, *et al.* Phenotypic profiling of CFTR modulators in patient-derived respiratory epithelia. *NPJ Genom Med* 2017; 2: 12.
- 40 Liu F, Zhang Z, Levit A, *et al.* Structural identification of a hotspot on CFTR for potentiation. *Science* 2019; 364: 1184–1188.
- 41 Veit G, Xu H, Dreano E, *et al.* Structure-guided combination therapy to potentially improve the function of mutant CFTRs. *Nat Med* 2018; 24: 1732–1742.
- 42 Capurro V, Tomati V, Sondo E, *et al.* Partial rescue of F508del-CFTR stability and trafficking defects by double corrector treatment. *Int J Mol Sci* 2021; 22: 5262.
- 43 Chin S, Hung M, Won A, *et al.* Lipophilicity of the cystic fibrosis drug, ivacaftor (VX-770), and its destabilizing effect on the major CF-causing mutation: F508del. *Mol Pharmacol* 2018; 94: 917–925.
- 44 Moran O, Galiotta LJ, Zegarrra-Moran O. Binding site of activators of the cystic fibrosis transmembrane conductance regulator in the nucleotide binding domains. *Cell Mol Life Sci* 2005; 62: 446–460.
- 45 Huang SY, Bolser D, Liu HY, *et al.* Molecular modeling of the heterodimer of human CFTR's nucleotide-binding domains using a protein-protein docking approach. *J Mol Graph Model* 2009; 27: 822–828.
- 46 Berkers G, van der Meer R, van Mourik P, *et al.* Clinical effects of the three CFTR potentiator treatments curcumin, genistein and ivacaftor in patients with the CFTR-S1251N gating mutation. *J Cyst Fibros* 2020; 19: 955–961.
- 47 Guhr Lee TN, Cholon DM, Quinney NL, *et al.* Accumulation and persistence of ivacaftor in airway epithelia with prolonged treatment. *J Cyst Fibros* 2020; 19: 746–751.